

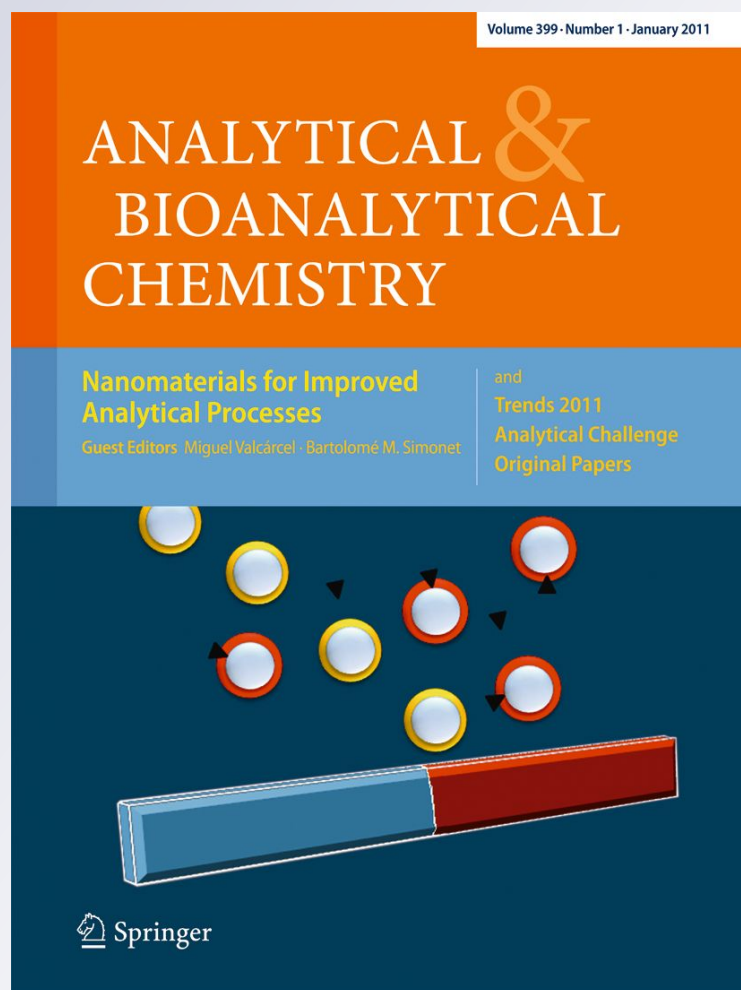
Physisorbed surface coatings for poly(dimethylsiloxane) and quartz microfluidic devices

*M. Viefhues, S. Manchanda, T.-C. Chao,
D. Anselmetti, J. Regtmeier & A. Ros*

**Analytical and Bioanalytical
Chemistry**

ISSN 1618-2642

Anal Bioanal Chem
DOI 10.1007/s00216-011-5301-z



Your article is protected by copyright and all rights are held exclusively by Springer-Verlag. This e-offprint is for personal use only and shall not be self-archived in electronic repositories. If you wish to self-archive your work, please use the accepted author's version for posting to your own website or your institution's repository. You may further deposit the accepted author's version on a funder's repository at a funder's request, provided it is not made publicly available until 12 months after publication.

Physisorbed surface coatings for poly(dimethylsiloxane) and quartz microfluidic devices

M. Viefhues · S. Manchanda · T.-C. Chao ·
D. Anselmetti · J. Regtmeier · A. Ros

Received: 24 May 2011 / Revised: 22 July 2011 / Accepted: 28 July 2011
© Springer-Verlag 2011

Abstract Surface modifications of microfluidic devices are of essential importance for successful bioanalytical applications. Here, we investigate three different coatings for quartz and poly(dimethylsiloxane) (PDMS) surfaces. We employed a triblock copolymer with trade name F₁₀₈, poly(L-lysine)-g-poly(ethylene glycol) (PLL-PEG), as well as the hybrid coating *n*-dodecyl- β -D-maltoside and methyl cellulose (DDM/MC). The impact of these coatings was characterized by measuring the electroosmotic flow (EOF), contact angle, and prevention of protein adsorption. Furthermore, we investigated the influence of static coatings, i.e., the incubation with the coating agent prior to measurements, and dynamic coatings, where the coating agent was present during the measurement. We found that all coatings on PDMS as well as quartz reduced EOF, increased reproducibility of EOF, reduced protein adsorption, and improved the wettability of the surfaces. Among the coating strategies tested, the dynamic coatings with DDM/MC and F₁₀₈ demonstrated maximal reduction of EOF and protein adsorption and simultaneously best long-term stability concerning EOF. For PLL-PEG, a reversal in the EOF direction was observed. Interestingly, the static surface coating strategy with F₁₀₈ proved to be as effective

to prevent protein adsorption as dynamic coating with this block copolymer. These findings will allow optimized parameter choices for coating strategies on PDMS and quartz microfluidic devices in which control of EOF and reduced biofouling are indispensable.

Keywords Static coating · Dynamic coating · Electroosmotic flow · Protein adsorption · PDMS · Quartz

Introduction

Microfluidics is a rapidly developing field with applications in molecular analysis, bioanalytics, or medicine [1–10]. These so-called lab-on-a-chip devices (LOC) assemble—depending on the detailed demands—miniaturized microreactors, separation systems, or detectors. Most often, they provide fast analysis of small quantities of analyte with high resolution [3, 4, 6, 7, 10–13]. In LOCs, surface properties become dominant because the surface-to-volume ratio increases drastically. As a consequence, control of surface properties is of utmost relevance to provide proper physical, chemical, and biological functions like the control of electroosmotic flow (EOF) or protein adsorption. This lack of control of the surface properties in LOCs has mostly prevented real-world applications [14].

There is a wide variety of materials used for microfluidic devices, e.g., silica, glass, and quartz or thermoplasts like poly(methyl methacrylate) (PMMA), polycarbonate (PC), poly(ethylene terephthalate) (PET), and cyclic olefine copolymer (COC) or elastomers like poly(dimethylsiloxane) (PDMS) [14–19]. Especially the latter is a frequently used material for LOCs. PDMS microchips are cheap, easy to fabricate (only the master wafer is fabricated in a clean room), and gas permeable (important for biological appli-

Electronic supplementary material The online version of this article (doi:10.1007/s00216-011-5301-z) contains supplementary material, which is available to authorized users.

M. Viefhues · D. Anselmetti · J. Regtmeier
Experimental Biophysics and Applied Nanoscience,
Bielefeld University,
33615 Bielefeld, Germany

S. Manchanda · T.-C. Chao · A. Ros (✉)
Department of Chemistry and Biochemistry,
Arizona State University Tempe,
Tempe, AZ 85287-1604, USA
e-mail: Alexandra.Ros@asu.edu

cations) [5, 20]. Disadvantages of PDMS comprise its hydrophobicity leading to unstable EOF, the high tendency to protein adsorption [21, 22], and consequently, its low reusability. In contrast, quartz LOCs are hydrophilic, reusable, and costly. In the UV spectral range, however, their transparency is unexcelled.

Miniaturized capillary electrophoresis in LOCs employs electric fields for the separation of analytes based on variations in their electrophoretic behavior. Simultaneously, the electric field induces transport of the liquid medium by EOF because of the charged channel or capillary surfaces. It is thus of utmost importance to control EOF for electrophoretic applications in LOCs to assure reproducibility and influence separation power. Generally, the electroosmotic mobility μ_{eo} can be approximated as [23]:

$$\mu_{eo} \propto \frac{\zeta \varepsilon}{\eta} = \frac{\sigma \lambda_D}{\eta} \quad (1)$$

where ζ refers to the zeta potential at the charged interface, ε to the permittivity of the medium, η to the viscosity, σ to the surface charge density, and λ_D to the Debye layer thickness. Equation 1 shows that μ_{eo} is proportional to the charges on the surface and inversely proportional to the solution viscosity. Most bioanalytical applications require defined buffers so that variations of the ionic strength to influence EOF are not applicable. In contrast, varying surface charges and the viscosity are means to control EOF for capillary electrophoresis applications [23–25].

For PDMS devices and to a lesser extent also for quartz, a number of surface modifications have been explored [20, 26]. Three main strategies for surface modifications are commonly employed. The first is the use of additives to the polymer formulation the device is made of, either as the basis for further surface-based polymerization reactions [27, 28] or to directly affect surface charges [29]. A second approach involves chemical or photochemical modification of the cured PDMS surfaces in which covalent bonds are formed between surface functional groups and reactive groups of the coating agents. Recent examples include UV-initiated grafting using different initiators [30–32] as well as chemical grafting of alkyne-PEG [33], polyethylene glycol monoacrylate, polyethylene glycol diacrylate [34], and immobilization of poly(L-glutamic acid) to PDMS [35]. These surface modifications are usually very stable but require specific functional groups on the microchannel surface targeting a reactive group of the coating agent. This approach is thus usually not applicable to different micro-device materials due to varying surface functional groups.

A third approach is modification by physisorption of charged or amphiphilic polymers and copolymers. Physisorption methods change surface properties fast and conveniently without chemical reactions involved [8, 9,

17, 36]. A disadvantage of physisorption methods consists in potentially weak interactions of the coating agents with the surface, which may lead to desorption and thus result in instable coatings.

In general, there are two strategies to apply physisorbed coatings: static and dynamic. In the first case, the coating is incubated for a specific time and then rinsed with pure buffer removing unbound residues. For dynamic coatings, the coating reagent is used in all solutions during an experiment. Therefore, if the coating substance partially desorbs, it may be replaced with coating molecules present in the used solution, thus overcoming the disadvantages of physisorption methods in case of weak interactions.

Compared to PDMS, surface coatings for quartz have been studied to a much lesser extent. However, due to its excellent optical properties, quartz remains a highly interesting material for LOCs. Recently, suitable surface coatings for quartz were investigated, such as the introduction of phospholipid polymers to modify EOF in a quartz microfluidic chip [26].

Here, we focus on physisorption of three different coatings on PDMS and quartz microchannel surfaces. We used F₁₀₈, poly(L-lysine)-g-poly(ethylene glycol) (PLL-PEG), and a mixture of *n*-dodecyl- β -D-maltoside and methyl cellulose (DDM/MC). PLL-PEG has a positively charged backbone; hence, it binds electrostatically to negatively charged surfaces [37–39]. F₁₀₈ is a triblock copolymer of poly(ethylene oxide)–poly(propylene oxide)–poly(ethylene oxide) (PEO–PPO–PEO) with flat (or “pancake”) conformation on hydrophilic, plasma oxidized PDMS [40]. The binding relies on the interactions between the hydrophilic PEO chains and the hydrophilic surface. DDM is an alkyl polyglucoside and belongs to the family of nonionic surfactants. The polysaccharide chain of MC has a high affinity to surface charges and binds via electrostatic interactions to the surface [36]. The chemical formulas of these compounds are shown in Fig. 1.

The coated surfaces were characterized by means of EOF measurements, contact angle, and protein adsorption with fluorescently labeled bovine serum albumin (BSA).

Materials and methods

Chemicals and reagents

Silicon wafers (p-type, doped with boron) were purchased from CrysTec (Germany). Negative photoresist SU-8 (50), SU-8 thinner GBL, and developer were obtained from Microresist (Germany). Tridecafluoro-1,1,2,2-tetra-hydro-octyl-1-trichlorosilane (TTTS) was purchased from Merck (Germany). Poly(dimethylsiloxane) (PDMS) (Sylgard 184) was from Dow Corning (USA). Glass microscope slides (76×26 mm) were obtained from Menzel (Germany). Quartz

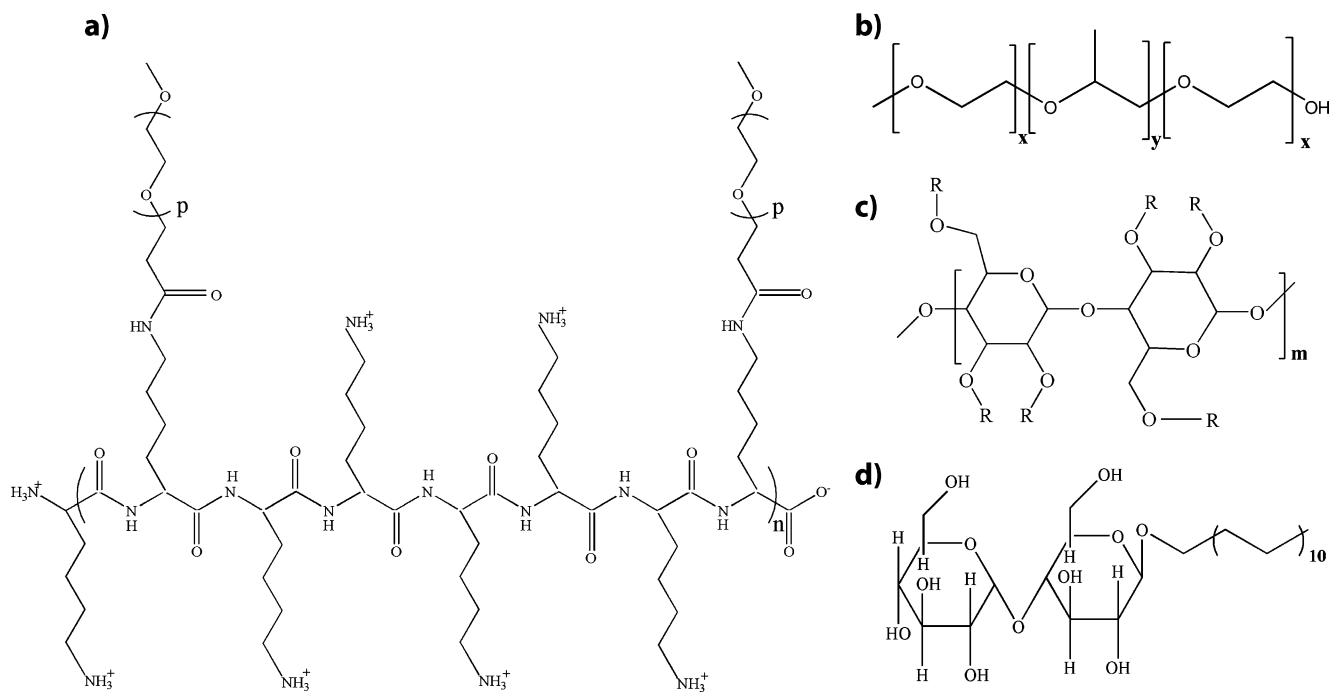


Fig. 1 Molecular structures of the surface coating agents employed in this study. **a** PLL-PEG ($n=19$, $p=113$). **b** Pluronic F₁₀₈ (with $x=132$ and $y=52$). **c** Methylcellulose. **d** DDM

glass chips were purchased from Capilix (Netherlands). Disodium hydrogen phosphate dihydrate was obtained from Fluka (Germany). POE-PPO-POE triblock copolymers F₁₀₈ (trade name Pluronic™) was a gift from BASF (Germany). DDM, methyl cellulose MC, and fluorescein isothiocyanate labeled BSA (FITC-BSA) were obtained from Sigma-Aldrich (Germany) and Alexa488-labelled BSA and Alexa488-labelled fibrinogen from Invitrogen (USA). Poly(L-lysine) (20)-g[3.5]-poly(ethylene glycol)(2) (PLL-PEG) was from SurfaceSolutionS (Switzerland). For all solutions, deionized water from a Milli-Q Biocel (Millipore, USA) was used.

Fabrication of poly(dimethylsiloxane) microfluidic devices

The PDMS microfluidic devices were fabricated via soft lithography, as previously reported [40, 41]. Briefly, the negative relief structure of the channels was created on a silicon wafer using contact lithography of SU-8 photoresist. This master wafer was silanized with TTTS. PDMS (pre-polymer and curing agent in ratio 10:1) was poured on the master wafer and cured at 85 °C for 4 h. After peel off, the PDMS slabs were cut, and reservoirs were punched to enable access to the channel. Right before chip assembly, the PDMS and a PDMS-coated glass slide were exposed to plasma oxygen in a home-built vacuum chamber [40] or a plasma cleaner (Harrick, USA). Dimensions of the linear micro channels were 20×20 μm² in width and height and 2 cm in length for PDMS chips. Quartz microchannels were

obtained from Capilix, Netherlands, at a length of 1 cm and a cross section of 30×30 μm².

Surface derivatization

Surface derivatization was either carried out in the PDMS and quartz microfluidic channels or on PDMS and quartz slabs. All quartz surfaces were rinsed with 0.1 M sodium hydroxide before treatment. Coatings were dissolved in phosphate buffer according to the measurement (see “Results and discussion” section). For PLL-PEG coating, 5 mg(mL)⁻¹ PLL-PEG (185 μM) was dissolved, hybrid DDM/MC coating included 2.5 μg(mL)⁻¹ DDM (0.25% (w/w)) and 0.3 μg(mL)⁻¹ MC (0.03% (w/w)), and F₁₀₈ coating was performed at a block copolymer concentration of 7.3 mg(ml)⁻¹ (500 μM). For static coatings, the surfaces were incubated for 30 min [37] and rinsed with buffer before measurements. For dynamic coating, the surface was incubated with coating agent for 5 min before the experiments were started. To perform the adsorption experiments, the initial incubation was followed by a second incubation step with a buffered solution containing the coating agent and protein.

EOF measurements

The electroosmotic mobility was determined according to the current monitoring method [42] and as previously reported [40]. Briefly, the decrease in current upon a buffer

exchange from a higher concentrated to a lower concentrated buffer was recorded to determine the electroosmotic mobility. We performed a buffer exchange from 20 to 18 mM phosphate buffer in the anode reservoir and recorded the current decrease at 500 V/cm applied via electrodes dipped in the reservoirs (power supplies from FUG (model HCN 14-12500 and HCN 7E-12500, Germany)). Voltage and current were controlled and recorded via a LabView program (National Instruments, USA). The electroosmotic mobility, μ_{eo} , was calculated with $\mu_{eo}=L^2/(Et)$, with channel length L , electric field E , and time t for complete exchange of buffer. The time was computed by calculating the point of interception of two linear fits applied to the monitored data. In case of PLL-PEG dynamic coating, the EOF was recorded with the same method, however, using a voltage sequencer from LabSmith (HVS448-6000D, LabSmith, USA). Polarity was reversed in the dynamic PLL-PEG case due to anodic EOF.

Contact angle measurements

For the advancing contact angle measurements, a goniometer (Krüss GmbH, Germany) was used. The surfaces were prepared accordingly to the coatings, whereas for the dynamic coatings, the surfaces were incubated for 30 min. After incubation, the surfaces were rinsed with pure buffer and dried with nitrogen. For each coating, the measurements were done at seven spots and averaged; the resulting error was $\pm 3^\circ$ at PDMS and $\pm 5^\circ$ at quartz surfaces.

Protein adsorption measurements

For the protein adsorption measurements, fluorescence intensity of fluorescently labeled BSA was determined on different derivatized surfaces. The surfaces were sectioned with PDMS slabs to avoid any mixture of coatings or washing agents. For the protein adsorption, a droplet of buffer with FITC-BSA (static) or, to mimic dynamic coatings, a buffer droplet containing BSA and coating agent were placed on the prepared surface and incubated for 30 min. In the dynamic case, the surfaces were additionally incubated with the coating agent for 10 min prior to protein adsorption. Fluorescence intensity was measured via fluorescence microscopy (inverted microscope (Axiovert 200, Zeiss, Germany) equipped with a mercury arc lamp (HBO50), CCD camera (Imager 3L, La Vision, Germany), and adequate filter sets). After rinsing the surface with buffer, the fluorescence intensity was determined again. The decrease of fluorescence was calculated with respect to the uncoated surfaces.

Experiments for the concentration dependence of coating agents were carried out with F_{108} and with Alexa488-BSA (Invitrogen, USA). A slightly different experimental set-up was used consisting of an IX71 inverted microscope

(Olympus, USA) and a QuantEM camera (Photometrics, USA). As we are reporting relative decreases in fluorescence intensities and not absolute values, a comparison to the above protein adsorption measurements with FITC-BSA is well justified. The concentration of F_{108} was varied from 2.5 μM to 10 mM, and incubations of the coating agent were carried out overnight. Alexa488-BSA was used at a concentration of 100 nM, and percentage values of the decrease were calculated in comparison to non-coated surfaces.

Results and discussion

In the following, we will present and discuss the effect of the three coatings physisorbed to PDMS and quartz surfaces. We particularly investigated the influence of dynamic and static coatings composed of the block copolymer F_{108} , PLL-PEG, and DDM/MC, as well as the static coating with PLL-PEG on the EOF in PDMS and quartz devices. In addition, we studied the prevention from protein adsorption and consequently biofouling for these coating strategies.

In our study, all PDMS surfaces were pretreated and activated with oxygen plasma to achieve reproducible starting conditions. In the literature, oxygen plasma treatment of PDMS is described to render it hydrophilic and increase electroosmotic mobility due to the creation of silanol groups on the surface [20, 22, 43, 44]. The quartz glass chips were rinsed with sodium hydroxide before measurements to increase silanol content on the surface in accordance with Ren et al. [22].

Effect of coatings on EOF

The effect of PLL-PEG, F_{108} , and DDM/MC coatings to the EOF in PDMS and quartz microchannels has been characterized by the current monitoring method [42]. Measurements of the EOF in uncoated microchannels served as references. The EOF was always directed from the anode to the cathode (positive EOF) [45, 46], except for the dynamic PLL-PEG coating. Table 1 shows the absolute and relative values for the electroosmotic mobility, μ_{eo} , which was influenced the most by the three dynamic coating methods. In fact, DDM/MC and the dynamic F_{108} coating both showed reductions of $>91\%$ in PDMS and quartz channels. Furthermore, the dynamic coating with PLL-PEG resulted in a reversal of the EOF direction (anodic EOF), thus a negative mobility. The static coating with PLL-PEG was effective to reduce EOF (83% in PDMS and 88% in quartz), however, less pronounced as in the dynamic cases of F_{108} and DDM/MC.

Our data obtained for the dynamic DDM/MC coating are in close agreement with the earlier reported reduction of nearly 100% for dynamic DDM/MC coated poly(methyl-methacrylate) (PMMA) microchannels [36]. Using only

Table 1 EOF mobility, μ_{eo} , of PDMS and quartz glass after different surface treatments

Surface derivatization ^a	$\mu_{eo} \times 10^{-4}$ [$\text{cm}^2(\text{Vs})^{-1}$]		EOF reduction ^b [%]	
	PDMS	Quartz	PDMS	Quartz
Uncoated	2.1±0.33	3.15±0.68	0	0
PLL-PEG (static)	0.36±0.05	0.38±0.08	83	88
PLL-PEG (dynamic)	-0.76±0.23	n.a.	Anodic EOF	n.a.
DDM/MC (dynamic)	0.13±0.02	0.28±0.09	94	91
F ₁₀₈ (dynamic)	0.14±0.02	0.26±0.06	93	92

^a PDMS surfaces were plasma oxidized before surface derivatization

^b Reduction is calculated relative to uncoated surfaces

DDM, however, as presented by Dang et al. [36] and Huang et al. [47], the EOF was only reduced by 25% in PMMA and 50% in PDMS channels [36, 47]. Two reasons are likely to pertain to the observed reduction in EOF: First, the increase of viscosity by methylcellulose [36] reduces EOF according to Eq. 1. Second, the surface charges are masked by the DDM coating [36, 47, 48]. In the case of PLL-PEG, masking of surface charges occurs as well and even leads to a polarity change on the surface so that the EOF direction is changed.

For F₁₀₈, we can directly compare the differences in dynamic and static coating for PDMS. Hellmich et al. determined a reduction of 50% of EOF for static F₁₀₈ coatings [40]. Here, we found a reduction of 93% for dynamic coating demonstrating, an effective advantage of dynamic coating versus static coatings. As a general finding in our study, channels treated with dynamic coatings exhibit stronger reduction in EOF compared to static coatings. In addition, the surface coatings had an influence on the quality of the EOF measurement. The reproducibility was improved for all coatings. For example, the standard deviations decreased from $0.33 \times 10^{-4} \text{ cm}^2(\text{Vs})^{-1}$ (PDMS) and $0.68 \times 10^{-4} \text{ cm}^2(\text{Vs})^{-1}$ (quartz) for uncoated surfaces to less than $0.1 \times 10^{-4} \text{ cm}^2(\text{Vs})^{-1}$ for coated surfaces.

An important aspect of surface coatings represents their stability during repeated applications as well as the long-term stability. We tested both of these properties for static PLL-PEG coating and dynamic DDM/MC coating in PDMS channels. First, we determined the short-term stability of electroosmotic mobilities consecutively several times in the same channel. No significant changes for the dynamic DDM/MC coating could be determined, whereas the electroosmotic mobility of the static PLL-PEG coating increased (Fig. 2).

To test the long-term stability, we recorded μ_{eo} of static PLL-PEG and dynamic DDM/MC coatings over 7 days. This was achieved by incubating PDMS chips once with PLL-PEG and subsequent EOF measurements at days 1, 3, and 7. For dynamic DDM/MC coating, the PDMS chip was filled with the coating solution, and EOF was quantified at the same time intervals as for PLL-PEG coated chips. For static PLL-PEG, μ_{eo} increases over 7 days from $(0.39 \pm$

$0.03) \times 10^{-4}$ to $(0.62 \pm 0.06) \times 10^{-4} \text{ cm}^2(\text{Vs})^{-1}$, whereas for dynamic DDM/MC, no significant increase was found (Fig. 3), i.e., the dynamic DDM/MC coating showed better long-term stability. Thus, a similar trend as for the consecutive repetition of EOF measurements was found confirming an overall higher stability, i.e., control of EOF with the dynamic coating method employing DDM/MC. This can be attributed to the regeneration of the coated surface by coating agents present in the dynamic procedure, which are able to occupy free areas on degraded surfaces. This finding is in good agreement with literature [47, 49]. Summarizing this section, the highest reduction of EOF could be observed on dynamically coated PDMS and quartz with F₁₀₈ or DDM/MC, and flow reversal was observed with PLL-PEG.

Contact angle measurements

The different coatings have further been investigated by goniometry. Table 2 summarizes the resulting contact angles before and after surface derivatization with DDM/MC, PLL-PEG, and F₁₀₈. Whereas native PDMS is highly hydrophobic, an advancing contact angle of $33 \pm 3^\circ$ was

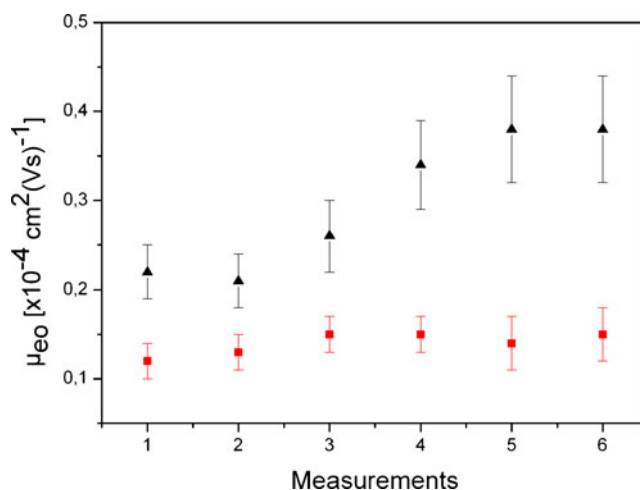


Fig. 2 Electroosmotic mobility of consecutive measurements for static PLL-PEG coating (black triangles) and dynamic DDM/MC coating (red squares) in PDMS channels. Indicated are the means for each measurements. Error bars indicate the standard deviation

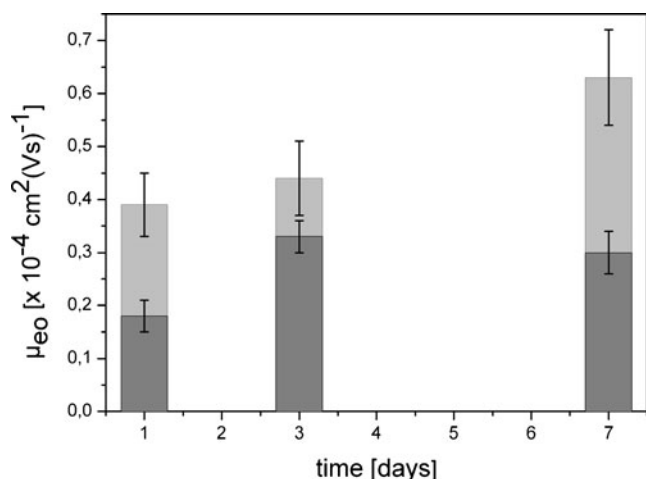


Fig. 3 Long-term measurements of static PLL-PEG coating (light grey) and dynamic DDM/MC coating (dark grey) in PDMS channels. The mean electroosmotic mobility calculated from five independent experiments is indicated. The error bars indicate the standard deviation

observed for plasma-oxidized PDMS. The increased wettability for plasma-oxidized surfaces is well documented in the literature [20, 40, 43, 44, 50]. The contact angle of uncoated quartz was determined as $34 \pm 5^\circ$ resulting as hydrophilic as plasma-oxidized PDMS. In literature, a contact angle of about 35° was reported for quartz surfaces, which is in good agreement to our results [51]. In summary, all coatings resulted in reduced contact angle in comparison to the native surfaces. Best wettability could be achieved on PMDS for DDM/MC coating with a contact angle of $12 \pm 2^\circ$.

Protein adsorption

Since protein adsorption and surface wettability have been shown to be closely correlated [20, 21], we next quantified the effects of surface coating on protein adsorption. We chose fluorescein isothiocyanate (FITC)-labeled BSA as a well-characterized albumin, known to adsorb readily to surfaces and exhibiting a high abundance in blood and plasma. It is thus a standard protein for testing nonspecific binding to surfaces [47].

Table 2 Contact angle of PDMS and quartz surfaces

Surface derivatization ^a	Contact angle	
	PDMS	Quartz
Uncoated	$33 \pm 3^\circ$	$34 \pm 5^\circ$
PLL-PEG (static)	$19 \pm 3^\circ$	$20 \pm 5^\circ$
DDM/MC (dynamic)	$12 \pm 2^\circ$	$10 \pm 2^\circ$
F ₁₀₈ (dynamic)	$16 \pm 2^\circ$	$12 \pm 2^\circ$

^a Plasma oxidization of PDMS surfaces before surface derivatization

First, we compared the reduction in protein adsorption for the coating concentrations used in EOF measurements. Table 3 shows the percentage of reductions of BSA adsorption observed for the different coatings. The decrease of protein adsorption was calculated relative to plasma-oxidized PDMS surfaces and sodium hydroxide rinsed quartz. The highest reduction of protein adsorption could be achieved with dynamic DDM/MC coating with $74 \pm 5\%$ and $79 \pm 5\%$ reduction on PDMS and quartz, respectively. Indeed, coatings with the highest wettability (smallest contact angle) demonstrated the smallest adsorption of BSA. For F₁₀₈ and PLL-PEG surface derivatization, the adsorption of FITC-BSA also decreased, however, to a lesser extent. Static PLL-PEG resulted in $45 \pm 3\%$ and $48 \pm 3\%$ on PDMS and quartz, respectively. Reductions of $59 \pm 5\%$ and $63 \pm 5\%$ were achieved with dynamic F₁₀₈ coating on PDMS and quartz, respectively.

Next, we compared our data with literature values. Dang et al. showed a reduced protein adsorption for DDM and MC coating on PMMA surfaces [36]. On metal oxide and PDMS surfaces, PLL-PEG was also reported to reduce non-specific protein adsorption [37, 39, 52, 53]. A reduction of protein adsorption for F₁₀₈ coating was reported for nonporous polymeric membranes, PMMA and PVC [54–56]. Our data on BSA adsorption are thus in good agreement with reported literature values.

In order to identify optimized coating conditions, we compared dynamic versus static coating for different concentrations of the coating agents. A priori, we expect a difference of these two coating methods, as a refreshing of the surface in the static case is not warranted during applications such as in capillary electrophoresis.

Starting with a static coating procedure, we varied the concentration of F₁₀₈ and tested the reduction of protein adsorption for various concentrations. Figure 4 shows the corresponding graph demonstrating a strong dependence of protein adsorption on the F₁₀₈ concentration. At a concentration above 1 mM, the reduction of protein adsorption reaches a plateau value of $\sim 80\%$. Below 1 mM, the

Table 3 Reduction of FITC-BSA adsorption

Surface derivatization ^a	Reduction of protein adsorption ^b [%]	
	PDMS	Quartz
Uncoated	0	0
PLL-PEG (static)	45 ± 3	48 ± 3
DDM/MC (dynamic)	74 ± 5	79 ± 5
F ₁₀₈ (dynamic)	59 ± 5	63 ± 5

^a Plasma oxidization of PDMS surfaces before surface derivatization

^b Reduction is calculated relative to uncoated surfaces

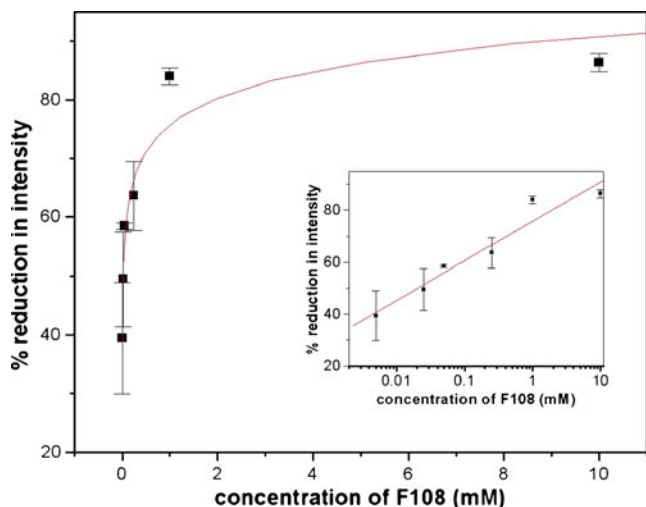


Fig. 4 Protein adsorption for varying concentration of coating agent F_{108} according to the static coating method: all values are averages of three independent measurements. The *line* shows a logarithmic fit to the data points as a guide to the eye. The *insets* show the same data set plotted logarithmically to demonstrate the values at low concentrations. *Lines in the insets* are linear fits. *Error bars* indicate standard deviation

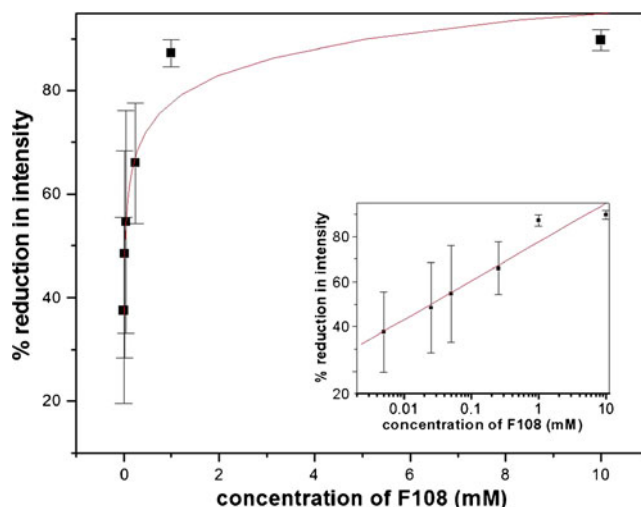


Fig. 5 Protein adsorption for varying concentration of coating agent F_{108} according to the dynamic coating method: all values are averages of three independent measurements. The *line* shows a logarithmic fit to the data points as a guide to the eye. The *insets* show the same data set plotted logarithmically to demonstrate the values at low concentrations. *Error bars* indicate standard deviation, and the *line in the inset* is a linear fit

reduction of protein adsorption decreases rapidly with decreasing concentration of coating agent.

Although BSA is a well-suited model protein to study protein adsorption, we further tested another blood borne protein with high adsorption tendency to surfaces. [Electronic Supplementary Material](#) to this manuscript shows the adsorption isotherm for fibrinogen adsorption on F_{108} -coated PDMS surfaces. Those are in very good agreement with BSA adsorption developing the saturation region at concentrations higher than 1 mM coating agent and similar maximal reduction of ~80% at these concentrations.

The dynamic coating procedure was tested by the following method. A pre-incubation step with the corresponding F_{108} concentration was executed first, followed by a dynamic procedure in which the surface was incubated with the same buffer containing both BSA and F_{108} . In an independent experiment, a time series at 1 mM F_{108} indicated that the maximum coating is already reached at 10 min (data shown in [Electronic Supplementary Material](#)), very well corresponding with the 5-min incubation time we used to compare the different coatings in Table 3. We thus tested the concentration dependence for the dynamic case at 10 min incubation time. As demonstrated in Fig. 5, a saturation region above 1 mM is observed corresponding to the previously observed static coating. Interestingly, the protein adsorption on PDMS using the dynamic coating procedure with PLL-PEG also showed a decrease in adsorption (see Fig. 6). However, the plateau value reached only ~80%. This could be attributed to a charge interaction of proteins with the positively charged PLL-PEG leading to

attraction forces. However, the reduction in protein adsorption was still quite high. Another interesting fact is apparent with PLL-PEG dynamic coating. The saturation concentration is three orders of magnitude lower than in the case of F_{108} . This can be explained by the fact that PLL-PEG has a high grafting density to PEG, whereas in F_{108} , only two PEG chains are apparent per molecule. Thus, a much lower

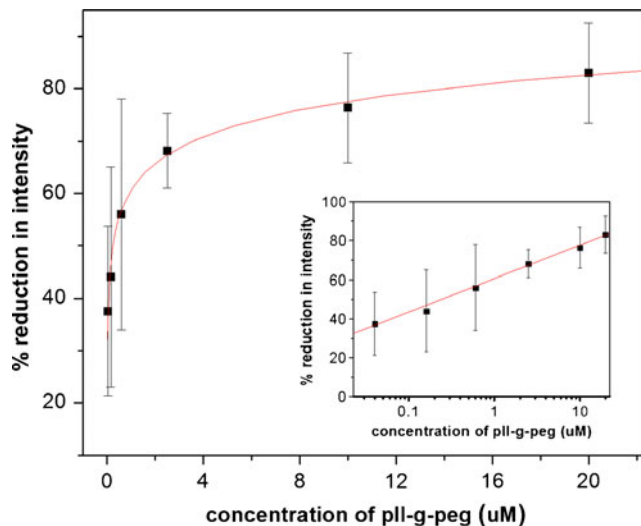


Fig. 6 Protein adsorption for varying concentration of coating agent PLL-PEG according to the dynamic coating method: all values are averages of three independent measurements. The *line* shows a logarithmic fit to the data points as a guide to the eye. The *insets* show the same data set plotted logarithmically to demonstrate the values at low concentrations. *Error bars* indicate standard deviation, and the *line in the inset* is a linear fit

concentration of PLL-PEG (but not PEG) can be employed to effectively reduce protein adsorption.

From both protein adsorption studies (static and dynamic), we found that the concentration used for all other measurements in our study are very close to the saturation regime, i.e., that a maximum coating efficiency is reached. This is also supported for the value of 59% from Table 3 for the reduction of protein adsorption at a F_{108} concentration of 500 μM corresponding well to the saturation value of 60% protein adsorption reduction we obtained from the isotherm in Fig. 5. Thus, we do not expect notable changes of the other parameters studied (contact angle, reduction of EOF) when increasing the coating agent concentration further.

Summary

We examined the effect of three coating agents on EOF, contact angle, and protein adsorption on poly(dimethylsiloxane) (PDMS) and quartz surfaces. PLL-PEG was used as static and dynamic coating, whereas F_{108} and the hybrid coating DDM/MC were employed as dynamic coatings. The electroosmotic mobility could be significantly reduced by all coating agents. The highest reduction was achieved for the dynamic coatings F_{108} and DDM/MC with reduction of more than 90% for both cases. For PLL-PEG, a reversal and thus anodic EOF was recorded. This interesting finding indicates that the surface could be titrated by the adequate amounts of PLL-PEG dynamic coating agent to null EOF. This is very advantageous for DC analytical applications, in which EOF is not desired. Moreover, the long-term stability and reproducibility of EOF were superior for dynamic coatings as compared to static coatings.

All surface coatings resulted highly hydrophilic on PDMS. Untreated quartz glass was as hydrophilic as plasma-treated PDMS. After surface coating, the contact angles of quartz surfaces decreased for all coatings relative to uncoated surfaces. On quartz, the highest hydrophilicity could be determined for static PLL-PEG and dynamic DDM/MC coating.

The adsorption of FITC-BSA was investigated via fluorescence microscopy. All coated surfaces exhibited lower protein adsorption than uncoated surfaces. A dynamic coating of both substrates with DDM/MC demonstrated maximal reduction of EOF and protein adsorption. Interestingly, PDMS surfaces often described as an inferior material, showed less EOF, better wettability, and also less protein adsorption as compared to quartz.

The optimal coating choice will be dependent on the application of the microfluidic device. If a static coating is more desirable because the polymers may interfere with the measurements, PLL-PEG was found to perform in satisfactory manner to reduce EOF (by 83% and 88% on PDMS

and quartz, respectively), but was less effective in the reduction of protein adsorption compared to the other dynamic coatings (45% and 48% reduction in PDMS and quartz). For dynamic coating procedures, DDM/MC and F_{108} performed equally well to control EOF. Additionally, a flow reversal with dynamic coatings of PLL-PEG may be desirable for applications in which electroosmosis has to be tuned in a specific direction relative to electrophoretic transport directions. For the reduction of protein adsorption, DDM/MC performed better than the other polymers at lower concentration. However, if the amount of coating polymer is not limited, all coatings are similarly efficient in adsorption prevention. In addition, the long-term stability of DDM/MC may be relevant for certain applications. Our study thus provides a guideline for investigators using PDMS and quartz microfluidic devices for bioanalytical applications.

Acknowledgements We thank Dominik Greif, Bielefeld University, for technical assistance. Financial support from the Deutsche Forschungsgemeinschaft within the collaborative research project SFB-613 (project D2) and the National Institute of Health under grant 1R21RR025826-01A2 is gratefully acknowledged. We also thank Lin Gan, Arizona State University, for help with figure preparation.

References

1. Arora A, Simone G, Salieb-Beugelaar GB, Kim JT, Manz A (2010) Latest developments in micro total analysis systems. *Anal Chem* 82:4830–4847
2. Salieb-Beugelaar GB, Simone G, Arora A, Philippi A, Manz A (2010) Latest developments in microfluidic cell biology and analysis systems. *Anal Chem* 82:4848–4864
3. Reyes DR, Iossifidis D, Auroux P-A, Manz A (2002) Micro total analysis systems. 1. Introduction, theory, and technology. *Anal Chem* 74:2623–2636
4. Auroux P-A, Iossifidis D, Reyes DR, Manz A (2002) Micro total analysis systems. 2. Analytical standard operations and applications. *Anal Chem* 74:2637–2652
5. Dittrich PS, Tachikawa K, Manz A (2006) Micro total analysis systems. Latest advancements and trends. *Anal Chem* 78:3887–3908
6. Vilkner T, Janasek D, Manz A (2004) Micro total analysis systems. Recent developments. *Anal Chem* 76:3373–3385
7. West J, Becker M, Tombrink S, Manz A (2008) Micro total analysis systems: latest achievements. *Anal Chem* 80:4403–4419
8. Dang F, Zhang L, Jabasini M, Kaji N, Baba Y (2003) Characterization of electrophoretic behavior of sugar isomers by microchip electrophoresis coupled with videomicroscopy. *Anal Chem* 75:2433–2439
9. Liu J, Pan T, Woolley AT, Lee ML (2004) Surface-modified poly (methyl methacrylate) capillary electrophoresis microchips for protein and peptide analysis. *Anal Chem* 76:6948–6955
10. Whitesides GM (2006) The origins and the future of microfluidics. *Nature* 442:368–373
11. Ohno K-I, Tachikawa K, Manz A (2008) Microfluidics: applications for analytical purposes in chemistry and biochemistry. *Electrophoresis* 29:4443–4453

12. Khandurina J, Guttman A (2002) Bioanalysis in microfluidic devices. *J Chromatogr A* 943:159–183
13. Sia SK, Whitesides GM (2003) Microfluidic devices fabricated in poly(dimethylsiloxane) for biological studies. *Electrophoresis* 24:3563–3576
14. Pallandre A, de Lambert B, Attia R, Jonas AM, Viovy J-L (2006) Surface treatment and characterization: perspectives to electrophoresis and lab-on-chips. *Electrophoresis* 27:584–610
15. Zhang X, Haswell SJ (2006) Materials matter in microfluidic devices. *MRS Bull* 31:95–99
16. Stjernström M, Roeraade J (1998) Method for fabrication of microfluidic systems in glass. *J Micromech Microeng* 8:33–38
17. Lai S, Cao X, Lee LJ (2004) A packaging technique for polymer microfluidic platforms. *Anal Chem* 76:1175–1183
18. Becker H, Gärtner C (2008) Polymer microfabrication technologies for microfluidic systems. *Anal Bioanal Chem* 390:89–111
19. Becker H, Locascio LE (2002) Polymer microfluidic devices. *Talanta* 56:267–287
20. Wong I, Ho C-M (2009) Surface molecular property modifications for poly(dimethylsiloxane) (PDMS) based microfluidic devices. *Microfluid Nanofluid* 7:291–306
21. Wu D, Zhao B, Dai Z, Qin J, Lin B (2006) Grafting epoxy-modified hydrophilic polymers onto poly(dimethylsiloxane) microfluidic chip to resist nonspecific protein adsorption. *Lab Chip* 6:942–947
22. Ren X, Bachman M, Sims C, Li GP, Allbritton N (2001) Electroosmotic properties of microfluidic channels composed of poly(dimethylsiloxane). *J Chromatogr B Biomed Sci Appl* 762:117–125
23. Grossman PD, Colburn JC (1992) *Capillary electrophoresis—theory and practice*. Academic Press, London
24. Hjerten S (1985) High-performance electrophoresis elimination of electroendosmosis and solute adsorption. *J Chromatogr* 347:191–198
25. Kuhn R, Hoffstetter-Kuhn S (1993) *Capillary electrophoresis: principles and practice*. Springer, Berlin
26. Yan Xu, Takai M, Ishihara K (2010) Phospholipid polymer biointerfaces for lab-on-a-chip devices. *Ann Biomed Eng* 38:1938–1953
27. Wu YZ, Coyer SR, Ma HW, Garcia AJ (2010) Poly(dimethylsiloxane) elastomers with tethered peptide ligands for cell adhesion studies. *Acta Biomater* 6:2898–2902
28. Mikhail AS, Ranger JJ, Liu LH, Longenecker R, Thompson DB, Sheardown HD, Brook MA (2010) Rapid and efficient assembly of functional silicone surfaces protected by PEG: cell adhesion to peptide-modified PDMS. *J Biomater Sci Polym Ed* 21:821–842
29. Xiao Y, Yu XD, Xu JJ, Chen HY (2007) Bulk modification of PDMS microchips by an amphiphilic copolymer. *Electrophoresis* 28:3302–3307
30. Schneider MH, Willaime H, Tran Y, Rezgui F, Tabeling P (2010) Wettability patterning by UV-Initiated graft polymerization of poly(acrylic acid) in closed microfluidic systems of complex geometry. *Anal Chem* 82:8848–8855
31. Yang LY, Li L, Tu Q, Ren L, Zhang YR, Wang XQ, Zhang ZY, Liu WM, Xin LL, Wang JY (2010) Photocatalyzed surface modification of poly(dimethylsiloxane) with polysaccharides and assay of their protein adsorption and cytocompatibility. *Anal Chem* 82:6430–6439
32. De Smet N, Rymarczyk-Machal M, Schacht E (2009) Modification of polydimethylsiloxane surfaces using benzophenone. *J Biomater Sci Polym Ed* 20:2039–2053
33. Zhang ZW, Feng XJ, Xu F, Liu X, Liu BF (2010) “Click” chemistry-based surface modification of poly(dimethylsiloxane) for protein separation in a microfluidic chip. *Electrophoresis* 31(18):3129–3136
34. Sugiura S, Edahiro JI, Sumaru K, Kanamori T (2008) Surface modification of polydimethylsiloxane with photo-grafted poly(ethylene glycol) for micropatterned protein adsorption and cell adhesion. *Colloids Surf B Biointerfaces* 63:301–305
35. Miyaki K, Zeng HL, Nakagama T, Uchiyama K (2007) Steady surface modification of polydimethylsiloxane microchannel and its application in simultaneous analysis of homocysteine and glutathione in human serum. *J Chromatogr A* 1166: 201–206
36. Dang F, Kakehi K, Cheng J, Tabata O, Kurokawa M, Nakajima K, Ishikawa M, Baba Y (2006) Hybrid dynamic coating with *n*-dodecyl-beta-D-maltoside and methyl cellulose for high-performance carbohydrate analysis on poly(methyl methacrylate) chips. *Anal Chem* 78:1452–1458
37. Huang N-P, Michel R, Vörös J, Textor M, Hofer R, Rossi A, Elbert DL, Hubbell JA, Spencer ND (2001) Poly(L-lysine)-g-poly(ethylene glycol) layers on metal oxide surfaces: surface-analytical characterization and resistance to serum and fibrinogen adsorption. *Langmuir* 17:489–498
38. Morgenthaler S, Zink C, Stadler B, Vörös J, Lee S, Spencer ND, Tosatti SGP (2006) Poly(L-lysine)-grafted-poly(ethylene glycol)-based surface-chemical gradients. preparation, characterization, and first applications. *Biointerphases* 1:156–165
39. Blättler TM, Pasche S, Textor M, Griesser HJ (2006) High salt stability and protein resistance of poly(L-lysine)-g-poly(ethylene glycol) copolymers covalently immobilized via aldehyde plasma polymer interlayers on inorganic and polymeric substrates. *Langmuir* 22:5760–5769
40. Hellmich W, Regtmeier J, Duong TT, Ros R, Anselmetti D, Ros A (2005) Poly(oxyethylene) based surface coatings for poly(dimethylsiloxane) microchannels. *Langmuir* 21:7551–7557
41. Regtmeier J, Duong TT, Eichhorn R, Anselmetti D, Ros A (2007) Dielectrophoretic manipulation of DNA: separation and polarizability. *Anal Chem* 79:3925–3932
42. Huang X, Gordon MJ, Zare RN (1988) Current-monitoring method for measuring the electroosmotic flow rate in capillary zone electrophoresis. *Anal Chem* 60:1837–1838
43. McDonald JC, Duffy DC, Anderson JR, Chiu DT, Wu H, Schueller OJ, Whitesides GM (2000) Fabrication of microfluidic systems in poly(dimethylsiloxane). *Electrophoresis* 21:27–40
44. Morra M, Occhiello E, Marola R, Garbassi F, Humphrey P, Johnson D (1990) On the aging of oxygen plasma-treated polydimethylsiloxane surfaces. *J Colloid Interface Sci* 137: 11–24
45. Lucy CA, Underhill RS (1996) Characterization of the cationic surfactant induced reversal of electroosmotic flow in capillary electrophoresis. *Anal Chem* 68:300–305
46. Chen W, Yuan J-H, Xia X-H (2005) Characterization and manipulation of the electroosmotic flow in porous anodic alumina membranes. *Anal Chem* 77:8102–8108
47. Huang B, Wu H, Kim S, Zare RN (2005) Coating of poly(dimethylsiloxane) with *n*-dodecyl-beta-D-maltoside to minimize nonspecific protein adsorption. *Lab Chip* 5:1005–1007
48. Luo Y, Huang B, Wu H, Zare RN (2006) Controlling electroosmotic flow in poly(dimethylsiloxane) separation channels by means of prepolymer additives. *Anal Chem* 78:4588–4592
49. Zhang J, Das C, Fan ZH (2008) Dynamic coating for protein separation in cyclic olefin copolymer microfluidic devices. *Microfluid Nanofluid* 5:327–335
50. He Q, Liu Z, Xiao P, Liang R, He N, Lu Z (2003) Preparation of hydrophilic poly(dimethylsiloxane) stamps by plasma-induced grafting. *Langmuir* 19:6982–6986

51. Lamb RN, Furlong DN (1982) Controlled wettability of quartz surfaces. *J Chem Soc Faraday Trans 1* 78:61–73
52. Michel R, Pasche S, Textor M, Castner DG (2005) Influence of peg architecture on protein adsorption and conformation. *Langmuir* 21:12327–12332
53. Marie R, Beech JP, Vörös J, Tegenfeldt JO, Höök F (2006) Use of PLL-g-PEG in micro-fluidic devices for localizing selective and specific protein binding. *Langmuir* 22:10103–10108
54. Liu VA, Jastromb WE, Bhatia SN (2002) Engineering protein and cell adhesivity using peo-terminated triblock polymers. *J Biomed Mater Res* 60:126–134
55. Balazs DJ, Hollenstein C, Mathieu HJ (2002) Surface modification of poly(vinyl chloride) intubation tubes to control bacterial adhesion: Teflon-like and pluronics. *Eur Cell Mater* 3:7–8
56. Govender S, Jacobs EP, Bredenkamp MW, Swart P (2005) A robust approach to studying the adsorption of pluronic f108 on nonporous membranes. *J Colloid Interface Sci* 282:306–313